Behavioral/Systems/Cognitive

Large-Scale Synchronized Activity during Vocal Deviance Detection in the Zebra Finch Auditory Forebrain

Gabriël J. L. Beckers and Manfred Gahr
Department of Behavioural Neurobiology, Max Planck Institute for Ornithology, D-82319 Seewiesen, Germany

Auditory systems bias responses to sounds that are unexpected on the basis of recent stimulus history, a phenomenon that has been widely studied using sequences of unmodulated tones (mismatch negativity; stimulus-specific adaptation). Such a paradigm, however, does not directly reflect problems that neural systems normally solve for adaptive behavior. We recorded multiunit responses in the caudomedial auditory forebrain of anesthetized zebra finches (*Taeniopygia guttata*) at 32 sites simultaneously, to contact calls that recur probabilistically at a rate that is used in communication. Neurons in secondary, but not primary, auditory areas respond preferentially to calls when they are unexpected (deviant) compared with the same calls when they are expected (standard). This response bias is predominantly due to sites more often not responding to standard events than to deviant events. When two call stimuli alternate between standard and deviant roles, most sites exhibit a response bias to deviant events of both stimuli. This suggests that biases are not based on a use-dependent decrease in response strength but involve a more complex mechanism that is sensitive to auditory deviance per se. Furthermore, between many secondary sites, responses are tightly synchronized, a phenomenon that is driven by internal neuronal interactions rather than by the timing of stimulus acoustic features. We hypothesize that this deviance-sensitive, internally synchronized network of neurons is involved in the involuntary capturing of attention by unexpected and behaviorally potentially relevant events in natural auditory scenes.

Introduction

Auditory systems are continuously stimulated by a barrage of sounds, only a few of which are relevant for adaptive behavior. One important cue used by neural systems to distinguish relevant events from irrelevant ones is probability of stimulus occurrence. Sounds that have been experienced frequently in recent history, and that thus may be expected, are less likely to require attention than sounds that deviate from recent stimulus statistics. How neural systems detect such deviant sounds remains poorly understood, but it is known that this context-dependent task is achieved preattentively, at least in part. Auditory neurons in cats (Ulanovsky et al., 2003, 2004) and rodents (Pérez-González et al., 2005; Anderson et al., 2009; Malmierca et al., 2009; von der Behrens et al., 2009; Yu et al., 2009; Antunes et al., 2010) habituate on short timescales to probabilistically recurring tones in a frequency-selective way [stimulus-specific adaptation (SSA)], so that responses are stronger when tones are deviant. This phenomenon is hypothesized to be involved in the "automatic" detection of deviant sounds in natural auditory scenes (Nelken and Ulanovsky, 2007). Furthermore, a large body of studies in humans has addressed a possibly related EEG phenomenon called "mismatch negativity" (MMN), which arises when a sound violates a regularity formed by repetitive auditory stimulation (Näätänen et al., 2001; Winkler, 2007). These findings notwithstanding, a considerable gap remains between the experimental designs to investigate deviance detection—usually involving fast sequences of unmodulated pure tones—and the detection of deviant, potentially relevant sounds in natural auditory scenes. Indeed, despite the vast literature on MMN, and the plethora of cognitive functions and psychiatric diseases to which it is linked (Näätänen, 2003; Näätänen et al., 2007), as well as the burgeoning interest in SSA, it remains unclear how the underlying mechanisms that cause such phenomena solve problems that perceptual systems face in real life (but see Winkler et al., 2003).

Here, we investigate auditory deviance detection in the context of a natural behavior. Zebra finches, *Taeniopygia guttata*, are group-living birds that produce up to tens of thousands of short-range contact calls per day (Beckers and Gahr, 2010). Thus, the auditory scene of these birds is rife with behaviorally meaningful stimuli that recur on short timescales. Although the songbird auditory forebrain has been studied extensively in terms of acoustic feature coding (Müller and Leppelsack, 1985; Theunissen et al., 2000; Grace et al., 2003; Cousillas et al., 2005; Nagel and Doupe, 2006; Amin et al., 2007; Meliza et al., 2010; Jeanne et al., 2011), much less is known about its sensitivity to short-term history of natural stimuli. We recently found in the medial auditory forebrain widespread depression of responses to call stimuli that recur at natural rates (Beckers and Gahr, 2010), but if and how such modulation underlies the detection of unexpected calls remains unclear.

Received Dec. 6, 2011; revised June 8, 2012; accepted June 15, 2012.

Author contributions: G.J.L.B. and M.G. designed research; G.J.L.B. performed research; G.J.L.B. contributed unpublished reagents/analytic tools; G.J.L.B. analyzed data; G.J.L.B. wrote the paper.

We thank Sue Anne Zollinger and the anonymous reviewers for comments on this manuscript.

The authors declare no competing financial interests.

Correspondence should be addressed to Gabriël J. L. Beckers, Department of Behavioural Neurobiology, Max Planck Institute for Ornithology, Eberhard-Gwinner-Strasse 6, D-82319 Seewiesen, Germany. E-mail: beckers@orn.mpg.de.

DOI:10.1523/JNEUROSCI.6045-11.2012

 0270-6474/12/3210594-15$15.00/0

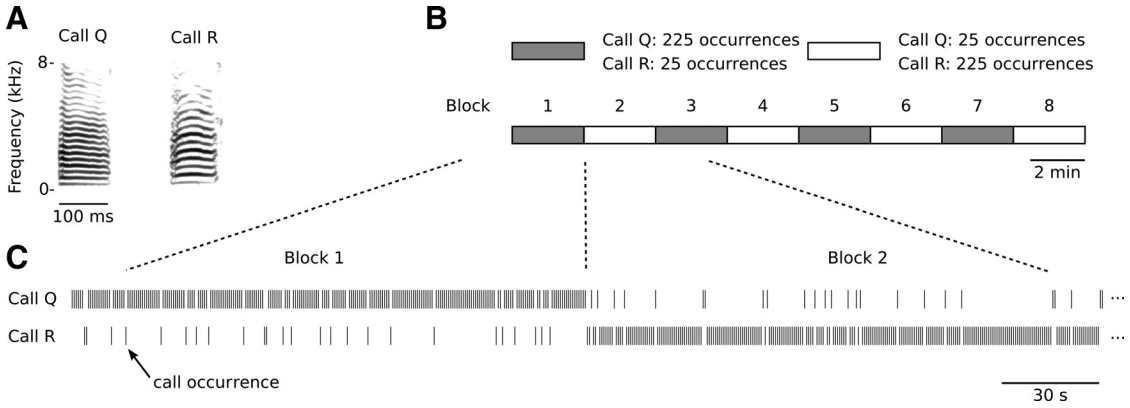

Figure 1. The switching-oddball stimulation paradigm used in this study. ***A***, Two representative short-range contact call stimuli that form the basis of a stimulation series. Call stimuli always originate from different individuals and are matched for duration and RMS level. ***B***, A stimulation series consists of eight blocks, in each of which both call stimuli are presented, but in different frequencies. One call stimulus is played 225 times (standard) and the other one is played 25 times (deviant); from one block to the next, these frequencies are reversed. Thus, overall call stimuli are played equally often, but their probability of occurrence alternates back and forth from 10 to 90% between blocks. ***C***, Calls are randomly intermixed so that call occurrences are probabilistic.

In the current study, we focus on this issue specifically and ask whether sites exist in the avian auditory forebrain that are preattentively sensitive to calls that deviate from those that are expected on the basis of recent history. To explore spatiotemporal activation patterns within and across functionally different areas, we use multielectrode probes and record analog multiunit activity (AMUA) within the auditory forebrain at 32 sites simultaneously.

Materials and Methods

Subjects. We used 12 adult (>120-d-old) zebra finches as subjects in this study. To avoid potential sex differences in auditory processing introducing heterogeneity in the results, all subjects were female. The birds were reared in a colony and housed in an aviary with other adult zebra finches of both sexes. Before recording, the animals had never heard the call stimuli used in this study, or any other vocalization of the animals from which they originate. All procedures were performed under systemic anesthesia under supervision of the institutional Tierschutzbeauftragte, in accordance with German laws and regulations (Tierschutzgesetz, §4, Absatz 3 and §§8b, 9 Absatz 2, Satz 2).

Acute recording. Birds were anesthetized with isoflurane gas (in oxygen; induction, 3%; maintenance, 1.5%), and then meloxicam (0.3 mg/kg; intramuscular injection) was administered for systemic analgesia. Subsequently, the bird's head was fixed in a custom-made stereotaxic frame while the body was resting on a heating pad to maintain body temperature. The setup allowed for electrophysiological recordings without ear bars, so that sound could freely reach the ears binaurally. After 20 min, the skull was exposed and a rectangular craniotomy was performed that extended from the area where the multielectrode probe would be inserted to the bifurcation of the midsagittal sinus, which acted as the coordinate reference point. An incision was made in the dura over the left hemisphere to accommodate parasagittal insertion of the multielectrode probe, between 0.3 and 0.8 mm lateral and centered around 0.8–1.2 mm rostral from the bifurcation of the midsagittal sinus. The tips of the shanks of the probe were positioned just above the brain surface so that it could be verified visually (magnification of stereomicroscope, 60×) that the head was fixed well and did not move due to breathing. The multielectrode probe was lowered in small steps to a position where the deepest shank reached a depth of 2500 μm below the brain surface. Probe placement was targeted to include the medial parts of field L, caudomedial nidopallium (NCM) and caudomedial mesopallium (CMM), but the extent to which these areas were sampled depended on the exact location of the probe, which differed between birds. In one individual (bird 7), we inserted the probe twice, the second time more medially than the first. We did not use any search stimuli. Playback of stimuli and electrophysiological recording started 30 min after the probe was in place.

We used six silicon-based multielectrode probes (Csicsvari et al., 2003; Blanche et al., 2005) of two types to record neural activity. Both probe types had four parallel shanks, each with eight electrode sites, but the spacing between shanks differed, being 200 μm for one type and 400 μm for the other. Distances between adjacent sites on a shank were always 200 μm (a4x8-5 mm200-200-413 and a4x8-5 mm200-400-413; shank thickness, 15 μm; electrode site surface, 413 μm^2; NeuroNexus Technologies). The resulting matrix of 8 × 4 recording sites thus extended over 1400 × 600 or 1400 × 1200 μm. The location of sites on the multielectrode probes is indicated by a tuple of two numbers, (*i*,*j*). The first number, *i*, stands for the shank on which a site is located, and ranges from 1 to 4, where 1 signifies the caudal-most shank and 4 the rostral-most shank. The second number, *j*, stands for the position of a site on a shank, and ranges from 1 to 8, where 1 signifies the top site that is nearest to the point where the shank penetrates the brain surface and 8 signifies the deepest site.

The 32 electrophysiological signals were referenced by a silver wire under the scalp and buffered by a headstage preamplifier (10× gain; MPA32I; Multi Channel Systems) before amplification with a multichannel amplifier (250× gain; fixed bandpass filters, 0.1–5000 Hz; PGA64; Multi Channel Systems). The amplified and filtered signals were digitized at 14 kHz and 16 bit resolution (NI9205; National Instruments) and stored on disk. To verify the precise temporal alignment of response epochs with the stimuli, we recorded with a microphone the call stimuli that were presented during the experiments and digitized the acoustic signal as an additional channel on the same data acquisition system.

Auditory stimuli. The 16 different stimuli used in this study (see example, Fig. 1*A*) are short-range contact calls that originate from 16 different male zebra finches. We operationally define a short-range contact call as the vocalization type that is produced most frequently by zebra finches in a social setting. Zann (1996) uses the term "tet-call" for those communication sounds that are produced as a "constant background" by wild zebra finches. However, in our laboratory recordings, the most frequently produced calls do not always conform to the described bioacoustic structure that has been reported for tet-calls. We therefore simply use "short-range contact call" for those calls that appear to function as such.

Eight call pairs were selected from a large database of call recordings from our laboratory (>10,000 calls per animal), with the criterion that calls within pairs had the same duration (difference, <1 ms) but differed in mean fundamental frequency sufficiently to be easily distinguishable by human listeners. To avoid extreme exemplars, a further criterion was that four acoustic feature measures (the first four statistical moments of the distribution of fundamental frequency measurements sampled at 1 ms intervals) of selected call stimuli should not deviate more than one quartile from the median, calculated from all short-range contact calls by the same individual. Detailed information on the recording and acoustic

analysis methods of call vocalizations are provided in the study by Beckers and Gahr (2010). The duration (range, 57–137 ms) and mean fundamental frequency (range, 380–716 Hz) of the call stimuli were as follows (call label, duration/mean fundamental frequency): E, 127 ms/551 Hz; F, 127 ms/433 Hz; G, 83 ms/413 Hz; H, 83 ms/570 Hz; I, 57 ms/470 Hz; J, 57 ms/530 Hz; K, 101 ms/564 Hz; L, 101 ms/470 Hz; M, 98 ms/462 Hz; N, 98 ms/603 Hz; O, 79 ms/509 Hz; P, 79 ms/451 Hz; Q, 109 ms/380 Hz; R, 109 ms/716 Hz; S, 137 ms/445 Hz; T, 137 ms/393 Hz.

During neurophysiological recording, calls were played at a level of 63 dB SPL at the head of the bird, as measured with a microphone (4190; Brüel & Kjaer) that was calibrated before use (4231; Brüel & Kjaer). The playback transducer (Vifa 10 BGS 119/8; Acoustic Systems Engineering) covered the perceptible frequency range of zebra finches (~0.4–10 kHz) and was positioned 0.5 m in front of the animal.

Experimental design. We played stimulus series that each consisted of two short-range contact calls, originating from different individuals. Within series, the two call stimuli were presented 1000 times each, according to a switching-oddball design (Fig. 1). A stimulus series was divided into eight continuous blocks of 250 call events, each containing 225 events of one call stimulus ("standard") and 25 of the other ("deviant"), which were randomly intermixed. Between consecutive blocks, the assignment of a call stimulus to standard or deviant conditions was switched. Thus, call stimuli were played equally often, but their probability of occurrence alternated between blocks. The time interval from call onset to the next call onset was 625 ms. The resulting call recurrence rate of the standard call falls within the range of spontaneous calling behavior in zebra finches (Beckers and Gahr, 2010). Individual birds received multiple series, each based on different call stimuli, but not all eight possible series were played to all birds (range, 1–7 series per bird; median, 5). The presentation order of the series was randomized for each individual.

Data analysis. Recorded electrophysiological signals were filtered offline to a high-frequency signal (0.5–5 kHz) containing action potentials, and subsequently rectified and decimated so that they reflect AMUA with a sampling period of 2.5 ms (see Fig. 2*A*). For the calculation of two measures (deviance preference and internal synchronization; see below), we applied a threshold to this signal, so that weaker firing from neurons that are farther away from the recording site was excluded from the signal by setting subthreshold samples to zero. The threshold was the same for all sites per recording, and was defined as five median absolute deviations above the median (both based on all samples from all sites pooled), with median absolute deviation defined as follows:

$$\mathrm{MAD} = \mathrm{median}(|\, a(t) - \mathrm{median}(a(t))\,|)$$

(Venables and Ripley, 1999). All data were stored in HDF5 files (version 1.8.4; http://www.hdfgroup.org), and analyses were performed in the scientific computing environment SciPy, version 0.8 (http://www.scipy.org/).

We defined response strength to a call event as the mean AMUA signal during a 500 ms call epoch that starts with the start of a call event. To exclude nonresponsive sites from our data set, we applied per call stimulus the criterion that the *z*-score difference in mean AMUA activity between the first 250 ms after call start and the next 250 ms should be >0.25, based on 100 deviant calls and 100 standard calls (last 25 standard events in each standard block) per series. The *z*-score difference is defined as follows:

$$z = \frac{(\mu_a - \mu_b)}{\sqrt{\sigma_a^2 + \sigma_b^2 - 2\mathrm{Covar}(a, b)}},$$

where a represents the mean AMUA signal during the first 250 ms and b during the next 250 ms, μ represents the mean, and σ represents its SD ($n = 200$). Responses may last longer than 250 ms, but visual inspection of raster plots suggested that, when this is the case, responses are generally strongest within the first 250 ms after call onset (call duration is ~100 ms). At primary auditory sites (see Results), where local activity is almost exclusively seen during auditory stimulation, the mean AMUA level during call stimulation is on average 2.9 times higher than the background level ($n = 361$ cases).

We are primarily interested in sites that respond more strongly to a call stimulus when it is deviant than to the same stimulus when it is standard. To identify such sites, we calculated for each call stimulus per site a "deviant preference" index (DP_C), defined as follows:

$$\mathrm{DP}_c = \frac{(d - s)}{(d + s)},$$

where d represents the mean response strength to a call stimulus when it is deviant (25 events in each of four blocks; $n = 100$), and s represents the mean response strength during the last 25 events of the same call stimulus in standard blocks ($n = 100$). A value of 1.0 indicates that a site only responds when the call is deviant, −1.0 indicates that it only responds when the call is standard, and 0.0 indicates no difference. Note that deviant and standard roles are switched seven times between consecutive blocks, so that modulation of response strength that does not covary with the local probability of a specific call, and hence does not alternate between blocks, will not be strongly reflected in this measure.

The term "deviant" in this paper refers to the fact that a call deviates from what may be statistically expected on the basis of recent stimulus history. The same property has been labeled "oddball," "rare," "improbable," or "novel" in the literature. "Deviance" is sometimes also used to refer to a hypothesized cognitive model in which a rare event violates a neural representation of expectation or prediction. However, we use the term strictly in a statistical sense.

Our results showed that activity patterns between secondary auditory sites are often synchronized. The degree of synchrony in AMUA activity between two sites, i and j, was determined by estimating their normalized cross-covariance. We used cross-covariance instead of cross-correlation because we were specifically interested in correlated firing that cannot simply be explained by the timing of the external stimulus (i.e., by two sites stereotypically responding to the same acoustic feature, or to different features that occur simultaneously). The cross-covariance between the AMUA activity of two sites, $a_i(t)$ and $a_j(t)$, as a function of τ, the time delay relative to $a_i(t)$, is given by the following:

$$C_{i-j}(\tau) = \frac{1}{T}\int_0^T \langle a_i(t) a_j(t + \tau)\rangle dt - \frac{1}{T}\int_0^T \bar{a}_i(t)\bar{a}_j(t + \tau) dt,$$

where T is the duration of the signal being analyzed (the duration of an epoch), $\langle\ \rangle$ indicates that the measure is averaged across epochs, and $\bar{a}_i(t)$ and $\bar{a}_j(t)$ are the time-varying mean firing rates of the sites (across epochs). The cross-covariance was estimated using the shuffle-corrected cross-correlogram method, as detailed in the study by Shaevitz and Theunissen (2007), where correlation in time-varying mean AMUA activity (i.e., the right side of the equation above), caused by direct stimulus effects, is estimated from the cross-correlation between sites with epoch order randomized according to a random permutation, and is subtracted from the overall cross-correlation (i.e., the left side of the equation above). In effect, the cross-covariance thus measures how deviations in the AMUA activity from the expected mean in site i are correlated with deviations in the AMUA activity from the expected mean in site j. The calculation of cross-covariance was based on 200 response epochs that consisted of a random 100 standard epochs and all 100 deviant epochs. We calculated cross-covariance between all site pairs per call stimulus, with τ ranging from −25.0 to +25.0 ms, in steps of 2.5 ms. Maximum cross-covariance was achieved most often at $\tau = 0$ ms (see Results). We therefore used the estimate of maximum cross-covariance between two sites as a measure for "internal synchronization" (IS).

Anatomy. Before implantation, the multielectrode probes were coated with the fluorescent dye DiI for later anatomical registration with histological sections. At the end of the recording session, the level of anesthetic (isoflurane) was increased to 5% to kill the animals, after which the brain was removed and frozen for cryostat sectioning (25 μm). One brain was lost in this process due to a technical problem with the cryostat, so that probe placement in this animal could only be determined on the basis of stereotaxic coordinates. For all other brains ($n = 11$), Nissl- or DAPI-

stained sections and fluorescence microscopy were used to verify probe location.

The zebra finch medial auditory forebrain consists of field L, NCM and CMM. The anatomy of field L in male zebra finches has been studied in detail (Fortune and Margoliash, 1992; Vates et al., 1996) and consists of different subfields: L, L2a, L2b, L1, and L3. There is no a priori reason to assume that the anatomy of the auditory forebrain in female birds would be different, but to our knowledge this has not been studied specifically. In the current study, most sampled sites in field L are situated medially and are either in L2a, or in L, which surrounds L2a in this part of the forebrain. Here, we do not distinguish between L and L2a because we are not able to do so on the basis of our histological material. L may not be distinct from L2b (Fortune and Margoliash, 1992), and the three subfields, L2a, L2b, and L, are therefore perhaps best referred to collectively as "L2," which is the term we will use here to refer to the medial ovoid structure of densely packed cells. In the part of the auditory forebrain that we sampled, the border between L3 and NCM is not distinct (Vates et al., 1996). Based on the anatomical descriptions in the study by Fortune and Margoliash (1992), we assume that the medial border of L3 occurs ~650 μm from the midline, but we are not able to detect it histologically in our sections. In two individuals (birds 9 and 12), the probe was located relatively laterally within the medial forebrain, so that it may have included a few sites in subfield L3, as well as a few sites in L1. In this part of the auditory forebrain, L3 is situated on the ventral border of L2a, while L1 is situated on its dorsal border (Fortune and Margoliash, 1992).

NCM is a relatively large area that we did not sample extensively; we predominantly sampled medial parts of NCM that are situated caudoventrally to L2, or medially to L2, and not dorsocaudal or lateral parts of NCM.

Statistics. The base data set in this study consists of AMUA measurements that have been performed per site ($n = 32$ simultaneously recorded sites per bird) during call epochs ($n = 1000$ per call stimulus per bird) of call stimuli ($n = 2$ per series) that were played in switching-oddball series ($n = 1$–7 series per bird; $n = 55$ in total) in different birds ($n = 12$). The main measures reported in this study have been calculated from the 1000 call epochs per stimulus for a given site, which we refer to as a "case." A stimulus series has thus 32 (sites) × 2 (call stimuli) = 64 of such cases.

For most statistical analyses, we used linear mixed models (LMMs), which were performed in R (R Development Core Team, 2009) (http://www.R-project.org), version 2.13.0. LMM was used with REML estimation, using the LMER procedure of the lme4 library (Baayen et al., 2008), version 0.999375-39, always with individual birds as a random factor. Fixed factors and the dependent variable are indicated in the text where results are reported. LMER provides a model of the observed data that can be evaluated for goodness of fit. When necessary, variables were log-transformed to meet the standard assumptions of normality of residuals and homogeneity of variances. Comparisons are reported as *t* statistics, with significance values computed using Monte Carlo Markov chain sampling with 10,000 iterations, as calculated by the pvals.fnc function of the languageR library (Baayen et al., 2008), version 1.2. Simultaneous measurements at different sites are not independent and are therefore averaged per auditory area (primary/secondary; see Results) before statistical analyses. Other statistics were performed using SciPy (http://www.scipy.org/), version 0.8.

Results

Response patterns are stereotypic in primary but variable in secondary forebrain areas

In the medial auditory forebrain, response patterns to different occurrences of the same call stimulus may be stereotypic or variable between events (Fig. 2*B*), in a way that is consistent with results from a previous study (Beckers and Gahr, 2010).

To quantify the level of such between-event stereotypy, we calculated for each site the mean normalized covariance between AMUA signals of the 1000 epochs per call stimulus (0.0 corresponds to a set of response patterns that are uncorrelated, 1.0 to perfect correlation). Figure 3 shows the mean response stereotypy values for every site in this study. Sites with strongly stereotypic responses (operationally defined as >0.5) are situated in, or near the border of, the thalamorecipient primary forebrain area L2. Sites in the secondary auditory areas CMM and NCM, which receive only weak direct thalamic input (Fortune and Margoliash, 1992, 1995), have a low response stereotypy (Fig. 3). Sites near the border between L2 and surrounding secondary areas, which in the medial part of the auditory forebrain is not distinct in our histological sections, often have intermediate stereotypy values. Sometimes, the AMUA response patterns of such sites are stereotypic but have a low amplitude. More often, however, they show both stereotypic and variable patterns at the same time, presumably because the multiunit signal in this border region contains action potential activity both from within and outside L2. Henceforth, we refer to sites with stereotypy values >0.5 as "primary auditory sites" (corresponding to the anatomical structure L2) and those <0.25 as "secondary auditory sites" (corresponding to NCM or CMM).

These observations on the anatomical distribution of response pattern stereotypy within the medial auditory forebrain not only confirm earlier findings (Beckers and Gahr, 2010) but also extend them because the current study includes sites that are situated more medially. Figure 3 shows that strongly stereotypic response patterns occur typically from ~400 μm lateral to the interhemispheric plane and beyond; closer to the interhemispheric plane, between 400 and 360 μm, stereotypic responses are rare (0.5% of the cases), and at 280 μm they are completely lacking. The transition around 400 μm lateral corresponds to the point where L2 has its medial border (Fortune and Margoliash, 1992).

Deviant call preference is high in secondary but low in primary auditory areas

When call stimuli recur in a switching-oddball series, response strengths in primary and secondary auditory areas are modulated in distinctly different ways.

Figure 4*A* shows an example of a primary site (L2) where response strengths to both call stimuli in the series decrease over time, for a considerable part already within the first 100 recurrences. At this site, activity is not strongly sensitive to call deviance, because, with respect to the overall variation, response strengths vary only weakly across block transitions. Accordingly, deviant preference values (DP_C) (see Materials and Methods) are low at this site for both stimuli: 0.01 and 0.05 for calls N and M, respectively. This example is typical for primary sites, which in general have low DP_C values (median, 0.06; $n = 361$ cases). We have previously shown that such response modulation at L2 sites to recurring calls is a short-term phenomenon, as it predominantly occurs at call recurrence intervals smaller than 5000 ms and is strongly dependent on the interstimulus time interval (Beckers and Gahr, 2010). This phenomenon can thus not be explained by a long-term memory effect, such as the one that has been found in NCM (Chew et al., 1996), which lasts for extended periods of time [i.e., many days (Phan et al., 2006)], and which is vocalization specific. These observations, together with the fact that, as in the example of Figure 4*A*, most primary sites in the current study respond to both calls in the switching-oddball series (88% of the cases), suggest that much of the response modulation in L2 can be explained by a form of short-term adaptation to acoustic features that are often shared between calls. Such modulation may be simply use dependent ("fatigue") (i.e., response levels decrease when neurons are stimulated more fre-

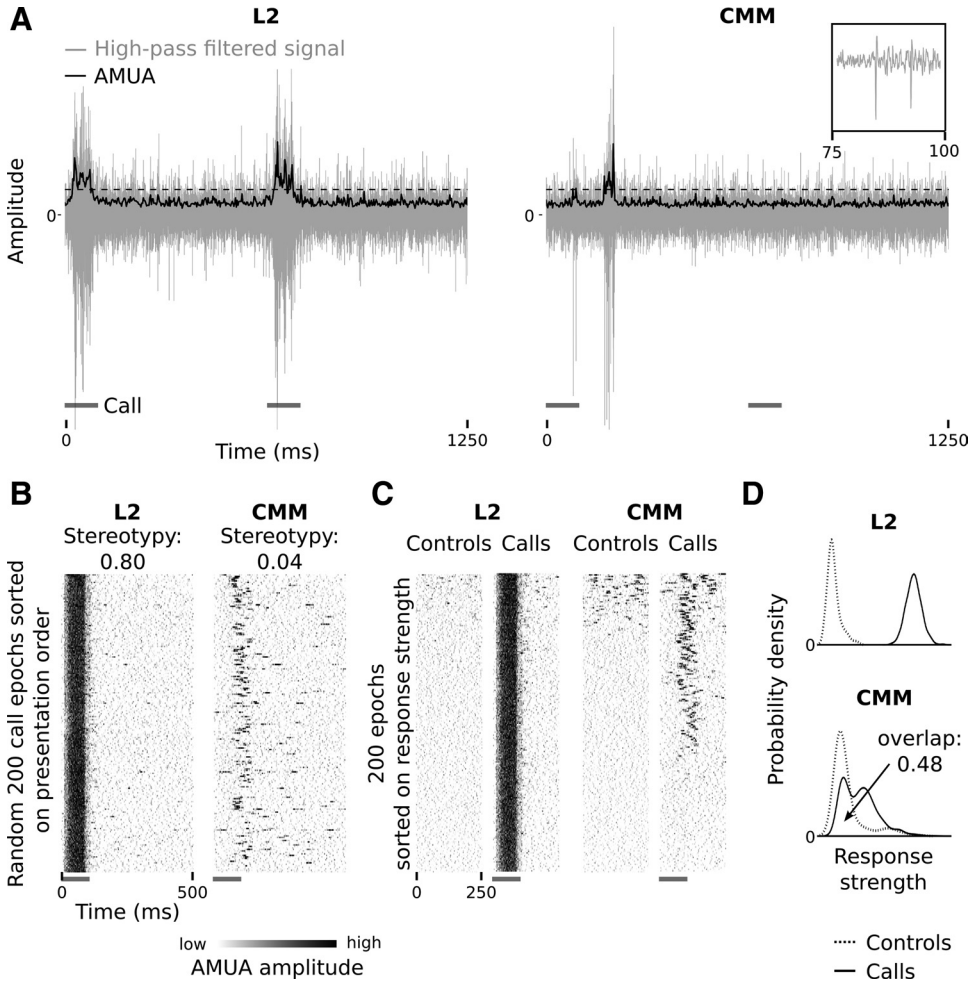

Figure 2. Examples of response properties to call stimuli in the primary auditory area L2 and the secondary auditory area CMM. L2 and CMM sites in these examples have been recorded simultaneously. The gray bars indicate call occurrences. ***A***, High-pass-filtered raw recordings (gray lines) are rectified and decimated to yield an AMUA signal (black lines) with a sampling period of 2.5 ms, which reflects the strength of local action potential activity. This signal has been used for most analyses in this study; in some analysis, an AMUA activity threshold was used (see Materials and Methods; here indicated with a dashed line). Shown are two consecutive response epochs, with time relative to the start of the first call in the example, not relative to the start of the call series. The inset shows two action potentials from the CMM signal. ***B***, Raster plots of a random 200 call epochs sorted on presentation order from top to bottom. Note that between-epoch response patterns are stereotypic in L2, and more variable in CMM. The dynamic range of these and other raster plots in this paper has been clipped for visual presentation only. ***C***, Responses during call epochs and silent control epochs (in which no calls were played). Raster plots are sorted on response strength from top to bottom. The call epochs are from the same events as in ***B***, but the sorting order is different. Note that approximately the lower third of the call epochs do not contain any response activity at the CMM sites, whereas the L2 site always shows response activity. Also note that control epochs may contain spontaneous activity. ***D***, Probability density plot of response strengths of call epochs and silent control epochs at the L2 and CMM sites of ***B*** and ***C*** ($n = 200$ epochs). In the L2 example, the curves do not overlap, which indicates that this site always responded to call stimulation. In the CMM example, there is a considerable overlap (0.48; the area under each curve is 1.0), which is caused by the site not always responding, as well as by spontaneous activity during silent control epochs.

quently) and is not compatible with a mechanism that distinguishes between standard and deviant calls.

Figure 4*B* shows an example of a secondary auditory site (CMM) that has been recorded simultaneously with the L2 site of Figure 4*A*. In contrast to the L2 site, response strengths at the CMM site covary with the short-term probability of the occurrence of specific call stimuli, which alternates between deviant and standard blocks. Corresponding to this pattern, DP_C values for this site are high: 0.47 and 0.52 for calls N and M, respectively. In the complete data set, DP_C values at secondary sites are variable, but generally much higher (median, 0.27; $n = 1890$) than those at primary sites. In a linear mixed regression model, the difference in DP_C between primary and secondary sites is highly significant (LMM; dependent variable, DP_C; fixed factor, site type; $t = 8.5$, $p < 0.0001$).

Crucially, the CMM site of Figure 4*B* responds to both call stimuli and has a high DP_C value for each of them. Figure 5 provides DP_C values for all secondary sites that respond to both call stimuli in a series (81% of 1890 cases) and shows that the level of deviant preference for call stimuli within a series is generally positively related. In contrast to the situation at primary sites, these observations cannot be directly explained by an adaptational mechanism that is based on a use-dependent decrease in response strength from frequent stimulation by an acoustic feature.

However, note that the responses in this study are based on multiunit signals. The responses in Figure 4*B* may thus represent the activity of two different, nearby neurons that each adapt strongly to a different acoustic feature that is not shared between the two call stimuli. However, this seems unlikely: the deviant sensitivity of the site in Figure 4*B* to both calls in the same series can also be observed at the simultaneously recorded 13 other secondary sites in this animal. All respond to both call stimuli, but predominantly only when they are deviant. Figure 6*A* shows a

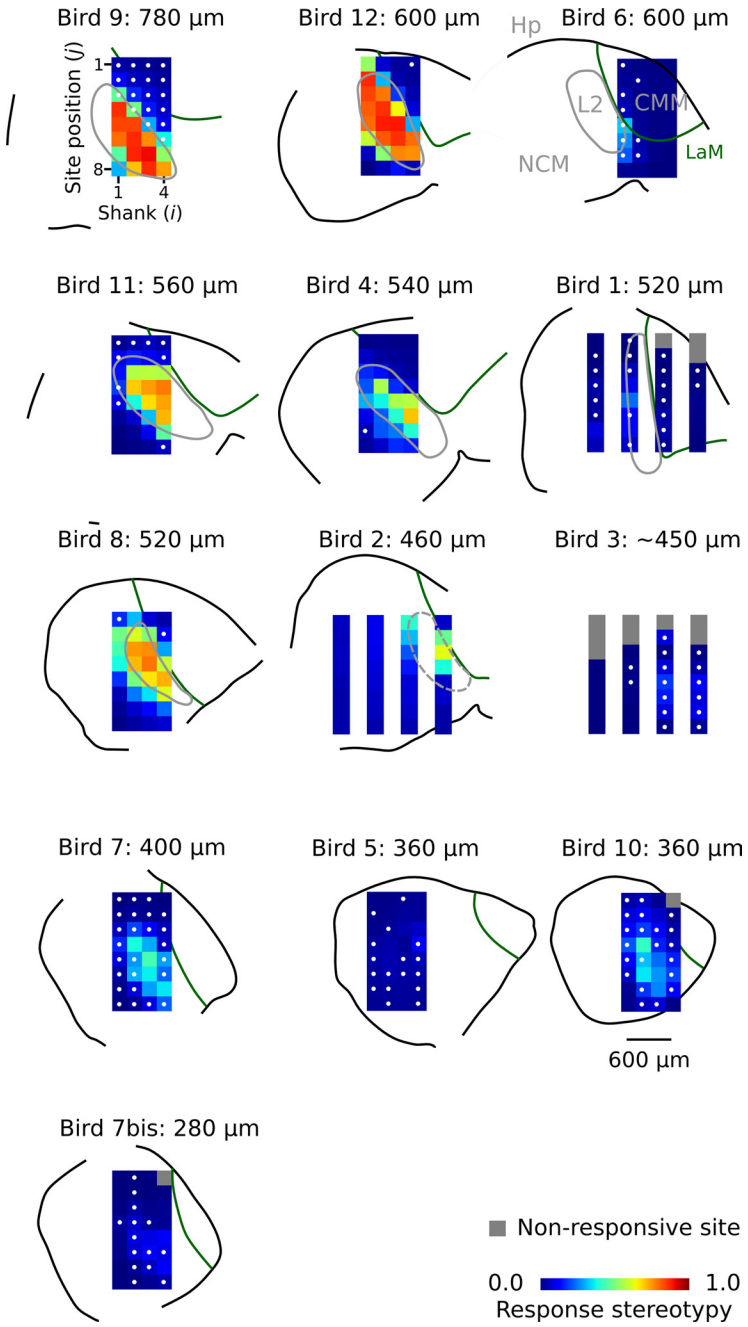

Figure 3. Locations of the multielectrode array in the auditory forebrain; this figure can be used as a map to identify the location of individual sites within auditory brain regions. Electrode sites are located at the center of the colored pixels in the 4×8 image matrix and are referred to throughout the text by a tuple of two numbers, (i,j), where i indicates the shank number and j, the site position on the shank. Colors represent the mean level of stereotypy, calculated over the different call stimuli that have been presented to each subject. Highly stereotypic responses are associated with the primary auditory area L2, while nonstereotypic responses are associated with secondary auditory areas NCM and CMM. For every individual, distance of the multielectrode to the interhemispheric plane is indicated, and the order of sections is organized from lateral (top left) to medial (bottom right). The location of the multielectrode in bird 3 could not be anatomically verified, and distance is based on stereotaxic coordinates. The interhemispheric and multielectrode planes are approximately, but not fully, in parallel. Distances to the midline have been estimated for the center of the array; the location of individual sites may thus deviate somewhat from this estimate in the medial–lateral direction. The white dots at pixel centers indicate that the corresponding site had DP_C values >0.25 for both call stimuli in at least one switching-oddball series. Orientation of the parasagittal sections is as follows: top, dorsal; bottom, ventral; left, caudal; right, rostral. The black outline caudodorsally indicates the border of nidopallium and mesopallium, not the brain surface. The solid gray lines indicate the border of L2; the dashed gray lines indicate that the border of L2 is indistinct. Hp, Hippocampus; NCM, caudomedial nidopallium; CMM, caudomedial mesopallium; L2, subdivision of field L that includes L, L2a, and L2b (between which we do not distinguish in the current study); LaM, lamina mesopallialis (Fortune and Margoliash, 1992; Vates et al., 1996). Note that the distance between the shanks in some multielectrodes may be either 400 or 200 μm.

raster plot of the site of Figure 4*B*, together with that of two of the simultaneously recorded sites and indicates their DP_C values, which are similarly high. DP_C values for the 11 sites that are not shown are as follows: (0.49, 0.57), (0.57, 0.51), (0.54, 0.60), (0.52, 0.52), (0.50, 0.45), (0.57, 0.29), (0.52, 0.47), (0.53, 0.45), (0.55, 0.43), (0.52, 0.45), and (0.55, 0.43). These sites are separated by distances between 200 and 1000 μm, which rules out the possibility that they reflect activity from the same neurons. Moreover, other call pairs recorded at the same site show the same pattern (Fig. 6*B*). Figure 6*C* provides additional raster plot examples of deviant-sensitive sites for six different animals.

How are such sites distributed over the different individuals and anatomical areas that we sampled? Applying a threshold criterion of DP_C values >0.25 for both call stimuli in a series, we find such sites in all but one individual (bird 2). The sites marked with a white dot in Figure 3 pass the criterion for at least one of the tested call series. From the spatial distribution, it is clear that such sites are not concentrated in one restricted area, but rather are distributed over much of the medial parts of the secondary auditory forebrain that we sampled, both in NCM and CMM.

Effect of short-term history

The positive DP_C values that we find for most sites could in principle be based on a "one-trial" effect: responses to a call are strong if the preceding call was different, but weak or absent if the preceding call was the same. This issue has been previously studied by investigating "local" sequences of stimuli (Squires et al., 1976; Ulanovsky et al., 2004). However, responses at secondary auditory sites in our stimulation paradigm can continue beyond the start of the next call event (Beckers and Gahr, 2010), which complicates the interpretation of sequence comparisons in general. Nevertheless, we can still rule out that the deviant preferences of the sites in this study are solely based on a one-trial effect. Figure 7 compares the mean response strengths of all secondary auditory sites to calls that are preceded by at least one deviant within the last 10 call events, and shows that standards that are immediately preceded by a deviant (DS) elicit a weaker response than deviants that are immediately preceded by another deviant (DD; LMM: $t = 5.0$, $p < 0.0001$). This is the opposite of what one would expect from a one-trial effect, even if response activity to a call may continue dur-

ing subsequent calls. Furthermore, there is only a very small difference between standards that are immediately preceded by a deviant (DS) and standards for which the last deviant was longer ago (DSS, DSSS, etc.), while a one-trial effect should lead to maximal differences. And last, there is a large difference between deviants with recency conditions 1250 and 1875 ms (i.e., DSD and DSSD) (LMM: $t = 3.1$, $p = 0.002$). A one-trial mechanism should produce similar responses to the last D because in both cases it is preceded by a S. If the one-trial change response additionally shows "overflow" into the next event, then DSD should produce a stronger response than DSSD, because the previous one-trial change occurred more recently. However, the opposite is the case: the 1250 ms recency condition leads to a significantly weaker response than the 1875 ms condition (Fig. 7). This shows that it is the recency of the occurrence of the previous deviant that weakens a deviance response, an effect that cannot be abolished by an intervening different call. The one-trial hypothesis can therefore be rejected, and we conclude that the increased response strength to deviant calls includes memory of previous call events beyond the most recent one.

Secondary auditory sites do not always respond to all call recurrences

In addition to a response bias to deviant calls, another interesting phenomenon that can be observed at secondary sites is that responses need not always occur. Figure 2*C* illustrates this phenomenon: we sorted the random 200 response epochs of Figure 2*B* on response strength instead of presentation order, and compared them with 200 control epochs. The primary site (L2) always shows a distinct response that is much stronger than the background level. The secondary site (CMM), in contrast, shows no event-related activity in approximately one-third of the call events. Note that some of the silent control epochs (approximately the top 35) at the CMM site contain "spontaneous activity" (i.e., activity not related to call events).

We did not attempt to algorithmically quantify the occurrence of nonresponses in our complete data set because it is problematic to quantitatively define a nonresponse in analog multiunit recordings that also contain spontaneous activity. Instead, we quantified the opposite, namely whether or not a site always responds, which can be done more reliably. Figure 2*D* shows the normalized response

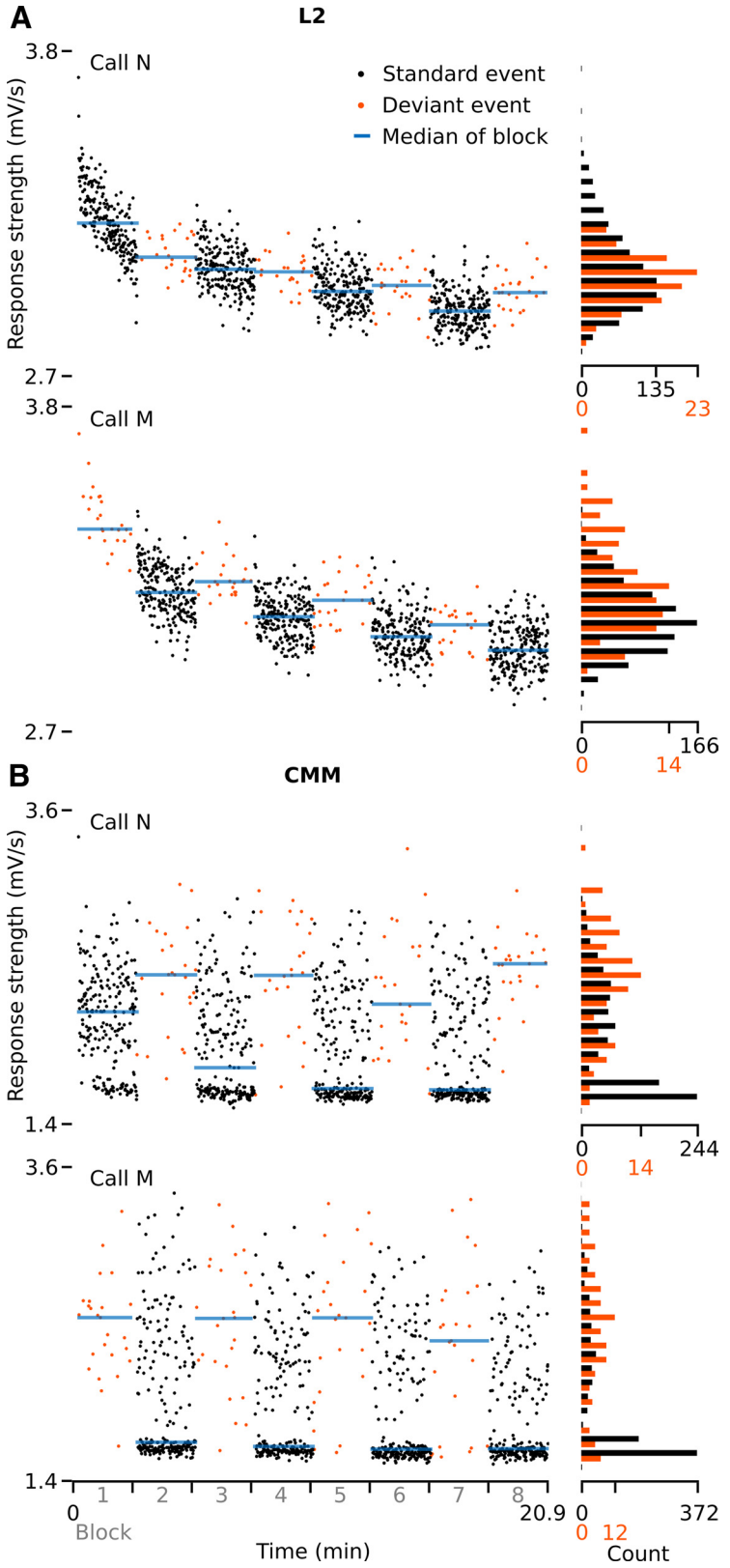

Figure 4. Examples of response strengths to individual call events in one switching-oddball series in bird 9. ***A***, ***B***, A site in L2, site (2,6) (***A***), and a site in CMM, site (3,3) (***B***). Sites have been recorded simultaneously. Every dot represents a stimulus presentation (event). Note that the histograms are normalized per condition (standard/deviant), which differ in the number of occurrences. The double-peak distributions in ***B*** are caused by the occurrence of nonresponses (lower peak) (i.e., "response" epochs that contain no AMUA activity above background level) (see Results, Secondary auditory sites do not always respond to all call recurrences).

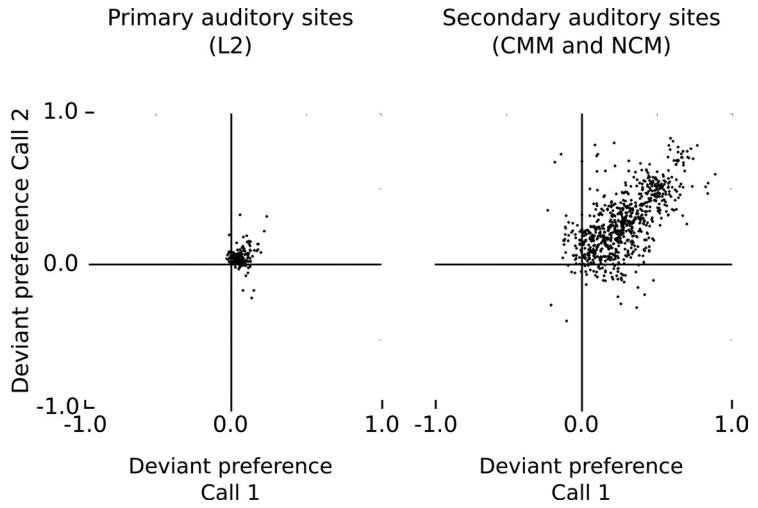

Figure 5. Relationship between deviant preference values, DP_C, of the two call stimuli within the same switching-oddball series for primary auditory sites (L2) and secondary auditory sites (CMM and NCM). Each dot represents the values of a call pair at a given site.

strength distributions of the L2 site in Figure 2*C*, for call and control events separately. There is no distribution overlap between calls and silent controls. This shows that the L2 site always responded to call events. For primary auditory sites, the proportional area of distribution overlap is 0.0 in the majority of cases (67% of 361 cases), and is very small in the remaining cases of it, having a median value of 0.03 (0.0 corresponds to no overlap, and 1.0 corresponds to identical distributions). Visual inspection of raster plots sorted on response strength showed that the very small amounts of distribution overlap that do occur are due to the rare occurrence of spontaneous activity in control epochs at primary sites, and never due to the lack of a response. Thus, even though response strength may decrease when call stimuli recur, we find that all primary auditory sites always respond to call stimulation in all birds, regardless of whether a call is standard or deviant.

The situation is markedly different at secondary auditory sites. The area of distribution overlap for the CMM site in Figure 2*C* is 0.48 (Fig. 2*D*). This is typical: for secondary auditory sites, the median overlap in response strength distributions between call response and control epochs is 0.45, with very few cases having no overlap (1% of 1890 cases). Such overlap may be caused both by a site not responding to part of the call events and by spontaneous activity during silent controls. We visually inspected raster plots sorted on response strength (compare Fig. 2*C*) of all secondary sites in our data set and found that overlap is often, at least partly, caused by responsive sites not responding to all call occurrences. Figure 8 provides for each individual bird a raster plot of a representative secondary site comparing 100 deviant call epochs to the 100 epochs with the lowest AMUA peak activity, and shows that sites may respond to some call occurrences and not to others, even though acoustic content is identical. Simultaneous response epochs of primary sites (Fig. 8) always show activity, indicating that auditory information does reach the primary auditory forebrain.

It should be noted that a "nonresponse" as described above means that no increased AMUA signal is observed within a time window that starts with call onset and lasts to the next call onset (i.e., 625 ms after the start of a ~100 ms call). In principle, we cannot rule out that responses are delayed to the extent that they occur later, during following call events. We have observed in a previous study that responses may last well beyond the onset of the next call (Beckers and Gahr, 2010), but in these cases activity already started during the epoch of the eliciting call event. Conversely, given that secondary sites are also active spontaneously, and that their responses to identical calls are rather variable, it should be noted that the presence of neural activity during a given call epoch does not necessarily indicate a response.

The high deviant preference values (DP_C) that we found for many secondary sites could be caused predominantly by a relatively high proportion of nonresponses to standard calls, or by lower (but not zero) activity levels to standard calls compared with deviant calls, or by both. To address this issue, we manually determined threshold levels to distinguish responses from nonresponses for one secondary site per bird. We did this on the basis of visual inspection of response strength histograms and raster plots [$n = 12$; responses at secondary sites are strongly correlated (see below), so that more sites per bird would amount to pseudoreplication]. Sites were selected for favorable signal-to-noise ratios and blindly with respect to the occurrence of nonresponses. Nonresponses were disproportionally rare at deviant events (in all 12 animals, deviants accounted for less than the a priori expected 10% of nonresponses, with a median of 2.8%). Next, we recalculated DP_C values for the selection of sites after removing nonresponse epochs. This led to a significant (LMM, $t = 8.9$, $p < 0.0001$) and large reduction of DP_C values, with the median decreasing from 0.27 to 0.07. Thus, the high DP_C values of secondary sites in this study can be largely explained by nonresponses occurring more often to standard events than to deviant events.

The mean percentage of nonresponses to standard events across animals was 37%, but there was considerable variation between birds in nonresponse levels, ranging from 10 to 75%. We determined whether or not nonresponses to standard events occur predominantly when they are preceded by a longer train of consecutive standard events (i.e., no recent deviant), but this turns out not to be the case: the mean percentage of nonresponses varies between 32 and 40% as the preceding number of consecutive standards varies between 0 and 9 (32, 39, 40, 38, 36, 36, 36, 37, 36, 37%, respectively). Thus, the occurrence of a deviant among the last few calls does not abolish nonresponses to standard calls, which points to a longer-term sensitivity of the mechanisms underlying this phenomenon to stimulus history statistics.

The finding that secondary sites need not respond to every call recurrence raises the question as to whether their low response stereotypy is caused primarily by call event epochs that lack responses, or whether responses, when they occur, are also variable in pattern (e.g., latency). We recalculated response stereotypy for all secondary sites, now basing it only on the subset of epochs that contained strong responses (defined as containing AMUA values of at least eight median absolute deviations above the median). Overall, this led only to a small increase in stereotypy values (mean increase, 0.01; SD increase, 0.03; $n = 1890$ cases), which confirms that at secondary auditory sites response patterns to recurring calls, when they occur, lack the strong between-event stereotypy that is observed at primary sites.

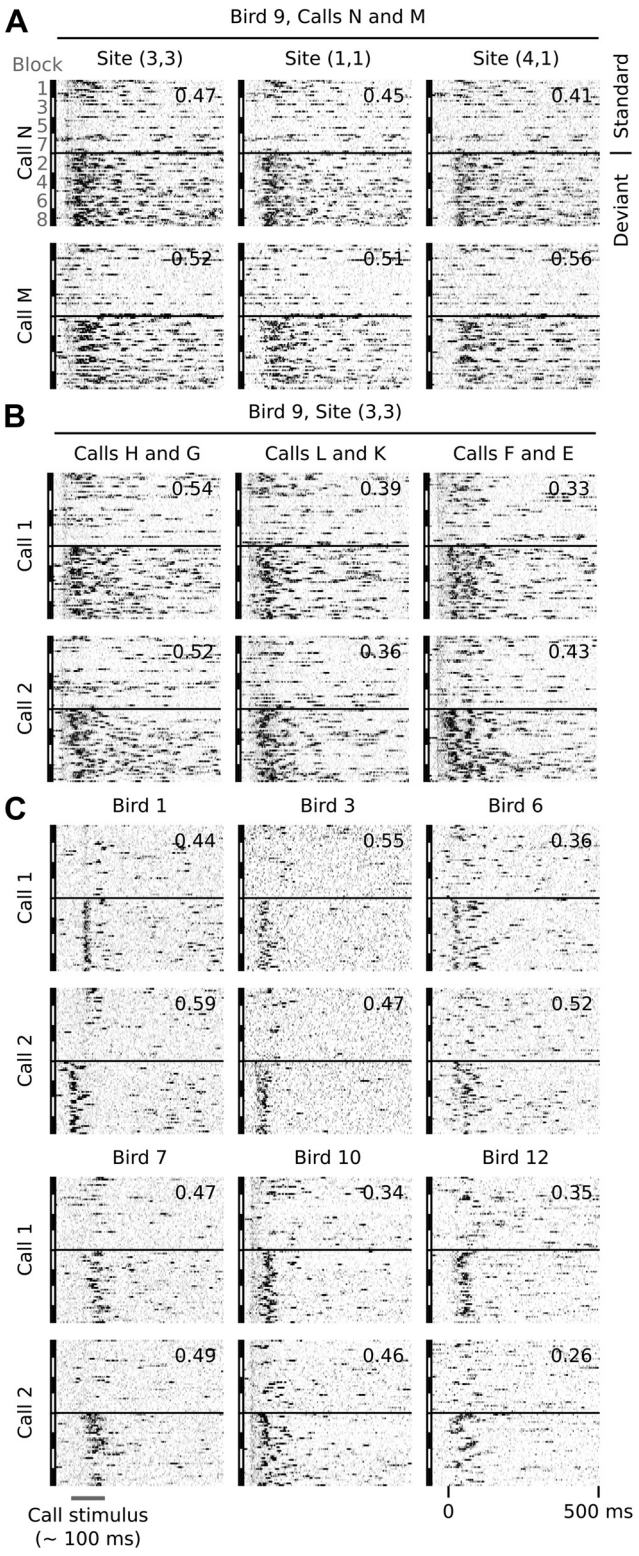

Figure 6. Examples of raster plots of AMUA activity at secondary auditory sites for standard and deviant conditions. Each raster represents one call stimulus within one switching-oddball series, where standard events (top; $n = 100$) and deviant events (bottom; $n = 100$) are vertically separated by a black line. Standard events were selected randomly (25 from 225 events per block). Deviant events are all represented (25 events per block). The numbers in the top right corner of each raster plot indicates the deviant preference value, DP_C, for that particular call and site. ***A***, Activity of two call stimuli, N and M, of one switching-oddball series recorded at three different sites simultaneously. Note that responses are biased to deviant events at all three sites. The same is true for the 11 other simultaneously recorded secondary sites in this animal (see text for DP_C values). Site (3,3) is the same site as shown in Figure 4*B*. ***B***, Activity to call stimuli of three other switching-oddball series in the same animal, at site (3,3). Responses at this site are biased to deviant events, regardless of the call stimulus. ***C***, Examples from six other birds: bird 1, site (3,5); bird 3, site (4,3); bird 6, site (1,1); bird 7, site (1,8); bird 10, site (2,8); bird 12, site (4,1).

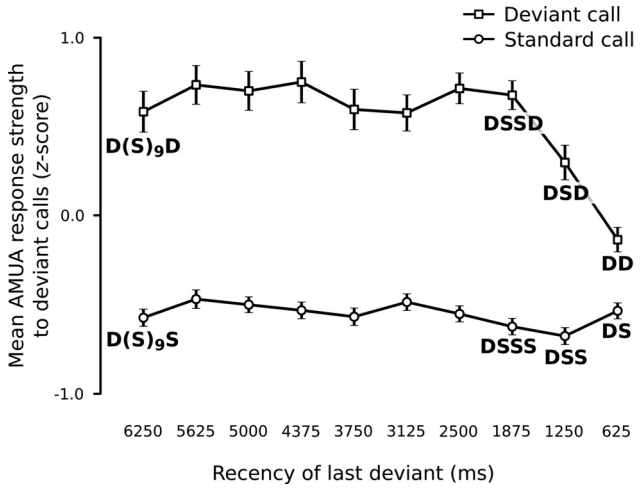

Figure 7. Responses of secondary auditory sites to deviant events are dependent on call event history beyond the immediately preceding call. For every recorded stimulus, call events were categorized according to the recency of the last deviant, between 625 and 6250 ms ago. As the call onset to next call onset interval was always 625 ms, recency 625 ms corresponds to those call events that were immediately preceded by a deviant, and recency 6250 ms are those for which the last deviant was 10 call events ago. *Z*-scores were calculated from the response strengths (mean of all secondary sites) to call events ($n = 2000$) within call series. The mean *z*-score ($n = 106$) and its SE are shown here per recency category and probability. D, Deviant; S, standard.

Responses of secondary auditory sites are internally synchronized

Although responses in secondary areas are considerably variable between call events, for the same event they are often remarkably similar between different sites. Figure 9*A* provides an example of this for two sites, (2,2) and (4,4), during a random selection of 20 call epochs from call stimulus Q in bird 10. Overall, the occurrence of activity is linked to the occurrence of the call stimulus, but response activity it is not precisely "locked" to that stimulus, as its latency varies considerably from event to event. Between sites, however, the variation in latency is strongly correlated so that responses virtually always occur synchronously. As this temporal correlation of event-related neural activity between sites cannot be explained by the timing of an external stimulus feature, or by the correlated occurrence of stimulus features, it must therefore represent a form of internal synchrony (Singer, 1999; Uhlhaas et al., 2009). We observe such internally synchronous responses at many secondary sites in virtually all raster plots of our data set.

To visualize synchrony in responses for the complete set of epochs from call Q in bird 10, we sorted raster plot rows on the latency of the strongest AMUA peak at site (2,2) (Fig. 9*B* illustrates this method for the subset of epochs shown in Fig. 9*A*). The raster plots of 13 other sites in Figure 9*C* have been aligned to that of (2,2) so that corresponding rows reflect concurrent activity in all raster plots. Although the other 13 sites are thus sorted on the latency of peak activity at site (2,2), and not on the latency of their own peak activity, they display the same pattern as the peak activity in (2,2), even when they are separated from (2,2) by large distances (>1000 μm).

←

In line with the internal synchronization of activity between these secondary sites, Figure 9*C* also shows that when site (2,2) does not respond within the 625 ms interval to the next call event, other sites do not respond either. These nonresponses occur throughout the switching-oddball series (Fig. 9*D*), which rules out the possibility that the secondary auditory forebrain simply stopped responding beyond some point in the series. Rather, large parts of the secondary auditory areas as a system do not respond to some call events, while resuming activity to subsequent events of the same call stimulus.

We initially wondered whether a technical artifact such as cross talk between channels in the recording setup could be responsible for the synchronicity of responses. However, this has been ruled out by comparing concurrent raw action potential signals between sites, an example of which is shown in Figure 9*E*. Sites are active simultaneously, but the action potential waveforms, on which AMUA signals are based, are different and therefore cannot originate from the same electrical source. Another possibility we considered is that the synchrony arises from a movement artifact due to breathing or heartbeat. However, we carefully checked for head and brain movement using a high-magnification stereomicroscope before and between recordings. Also, it is difficult to see how breathing or heartbeat could be completely absent (nonresponses) specifically during many, or in some animals during most, standard events. And, last, the level of internal synchronicity is much lower at primary sites than it is at secondary sites (see below), while both types are recorded in parallel with the same probe having fixed electrode sites (i.e., sites can physically not move independently from each other). Together, this renders the possibility of movement artifacts underlying the synchronously spiking bursts very unlikely and confirms a neuronal origin. Furthermore, it should be noted that the synchronized activity peaks visible in Figure 9*C* cannot be strictly a manifestation of a noninformation coding phenomenon. This must be so because the peaks do not occur randomly with respect to call stimuli, but tend to occur during or immediately after a call stimulus, causing the nonlinear shape in the distribution of activity peaks in the latency-sorted raster plots (Fig. 9*F*).

Internal synchronization of secondary sites over large distances is also present in other birds. Figure 10*A* provides examples from seven additional individuals. These representative site pairs have been selected not for maximum synchrony, but rather for high distance. Note that the two examples comparing CMM and NCM sites (birds 1 and 11) also show synchronous activity.

We investigated the extent of response synchronization for our complete data set by calculating for every possible site pair per call stimulus the level of cross-covariance of simultaneously recorded responses (see Materials and Methods) as a measure of internal synchrony (IS = 0.0 corresponds to no internal synchrony, IS = 1.0 to perfect synchrony, and IS = −1.0 to perfect antisynchrony). For comparison, IS for the site pair (2,2) and (1,2) in Figure 9 is 0.71, and that for (2,2) and (3,8) is 0.36, with the distances between these sites being 200 and 1217 μm, respectively. Note that IS values capture all internally synchronized activity during call epochs, not only the peak activity that is used for visualizing the phenomenon in Figures 9*C* and 10*A*.

For every site in our data set, there are 31 IS values per call stimulus, which is unwieldy for visual representation. Because we are primarily interested in (1) how many sites show internal synchrony with other sites, (2) whether or not many sites are involved in the same synchronous network activity, and (3) whether or not distant sites are part of such networks, we derived

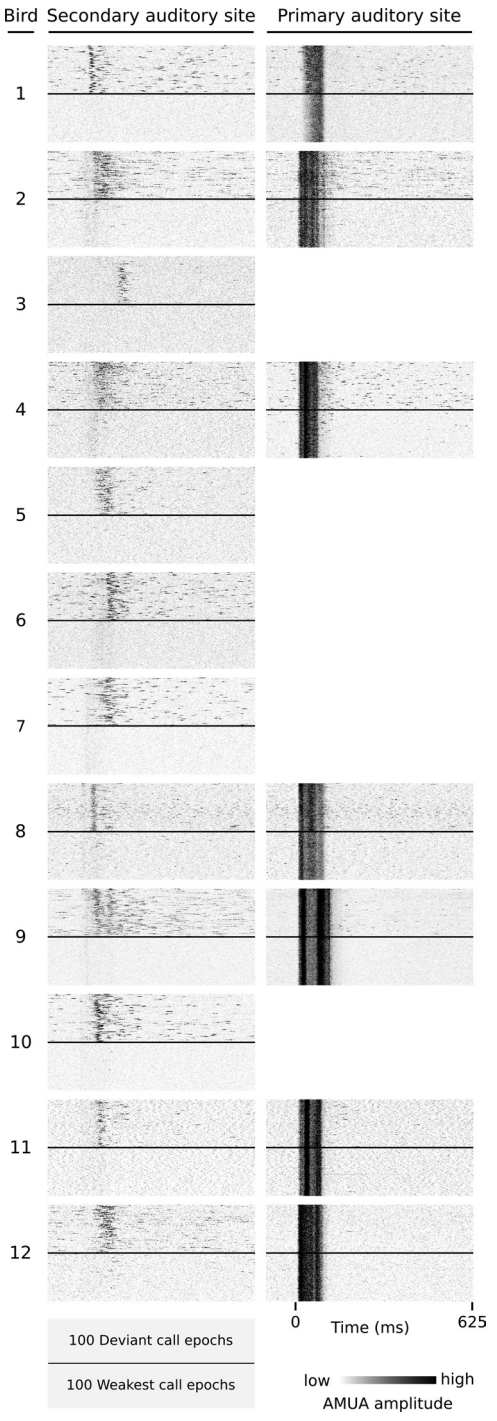

Figure 8. Examples of secondary auditory sites that do not always respond to call events. Each raster plot represents response epochs from one site; the top half are all 100 deviant events; the bottom half are the 100 epochs (of all 1000) with the weakest response strengths at the secondary site (first column). The second column shows the simultaneously recorded responses at a primary site, if available. Note that the 100 weakest epochs in the first column lack any response activity, while primary sites always respond. Bird 1: sites (3,8), (2,5); bird 2: (2,2), (4,3); bird 3: (2,4); bird 4: (1,8), (4,6); bird 5: (2,8); bird 6: (1,4); bird 7: (2,2); bird 8: (3,1), (3,2); bird 9: (2,2), (3,8); bird 10: (1,1); bird 11: (1,1), (4,4); bird 12: (4,1), (2,5). The L2 site of bird 1, (2,5), is situated on the border with NCM and has for most call stimuli a low stereotypy value (Fig. 3). The call shown here is an exception (stereotypy, 0.73), so that we classify it as a L2 response.

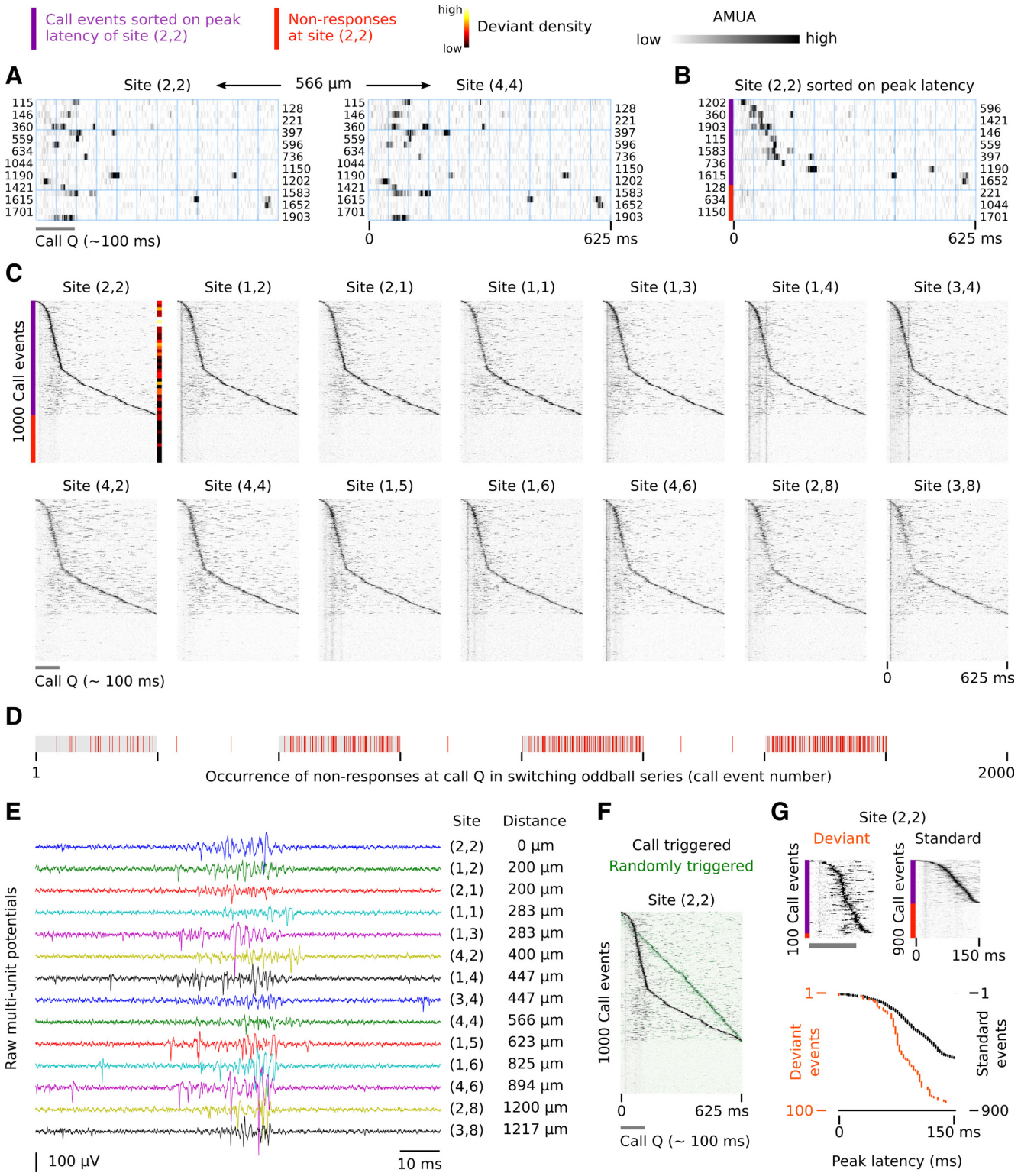

Figure 9. Internal synchrony in response patterns across different secondary auditory sites in NCM. ***A***, Raster plot of activity at two sites during a random 20 (of 1000) call epochs (call Q; bird 10). The numbers at the rows refer to the sequence number of the call event in the switching-oddball series. Activity patterns are similar between the two sites, which are 566 μm apart. ***B***, Same epochs of site (2,2) as in ***A***, but now sorted on the latency of the strongest peak within an epoch. Nonresponses (red bar) are considered to have no latency and are appended after the epoch with the longest latency. ***C***, The raster plot of all 1000 call Q epochs at site (2,2) is sorted on the latency of the strongest peak within an epoch, and the raster plots of the 13 other sites are ordered correspondingly, so that concurrent epochs are aligned vertically with that of (2,2). The peak of activity at (2,2) is matched by synchronous activity at other sites, even though it is not locked to the call stimulus. At a number of sites, response traces can be seen that are synchronized to the call stimulus, but these are faint and presumably originate from nearby primary sites in L2. The local density of deviants in the sorted raster is indicated by a color bar and has been calculated with a histogram using a bin width of call 50 epochs. Site (2,2) has a DP_c value of 0.30 for call Q and 0.26 for call R and is thus strongly sensitive to call deviance. ***D***, Nonresponses occur throughout the switching-oddball series and are followed by responses. Note that only nonresponses at call Q are indicated; the other call in the series (call R) is not shown. ***E***, Raw action potential waveforms around one peak at the different sites. The distances indicated are relative to site (2,2). ***F***, The nonlinear shape of the peak activity bursts in the call stimulus-triggered, latency-sorted rasters indicate that the underlying process that generates this activity is linked to call perception. If activity were (*Figure legend continues.*)

three mean IS values for each site that reflect these properties. We calculated "best internal synchrony," IS_B, which is the mean of the four highest IS values that a site has with any of the other sites. A site with a high IS_B value has synchronized activity with at least some other sites, but not necessarily with many and not necessarily with ones that are very distant (although the minimum average distance to four other sites is still at least between 200 and 362 μm, depending on the location of the site on the multielectrode probe). "Distributed internal synchrony," IS_D, is the mean of the 16 highest IS values, which makes it sensitive to the size of the synchronized network of which a site is a component. A site with a high IS_D value must have synchronized activity with more than a few sites. "Long-distance internal synchrony," IS_L, is the mean of the four highest IS values with sites that are >600 μm away. Figure 10*B* provides the mean IS_B, IS_D, and IS_L values for every site in this study and confirms our visual observations that virtually all secondary sites show considerable levels of internally synchronized activity (for the anatomical location of these sites, see Fig. 3). Primary sites, in contrast, show much lower IS values (median IS_B for primary and secondary sites is 0.18 and 0.48, respectively, a difference that is highly significant: LMM, dependent variable IS_B, $t = 10.9$, $p < 0.0001$). Most sites with a high IS_B value also have high IS_D values, indicating that such synchronization occurs on a large scale, and they also have high IS_L values, indicating that sites separated by >600 μm are part of the same synchronized network. Thus, internally synchronized response patterns to call vocalizations are the norm for secondary auditory areas in our recordings.

Time lags between signals to achieve maximal between-site correlation are on average very small (Fig. 10*C*): 73% of the cross-correlations between secondary sites were maximal without any time lag, while if time lags of 2.5 ms were allowed, the percentage increased to 89% of all cases (note that AMUA signals have a sampling period of 2.5 ms). Figure 10*C* shows the time lags at maximal cross-correlation for sites pairs that are at most 600 μm apart, and compares it with that of sites farther than 600 μm apart: the group with more distant sites generally have slightly higher time lags, but still 84% of all cases have lags of maximally 2.5 ms. This small difference may be explained by an increase in latency differences between correlated activity of sites that are farther apart, but also by a decrease over distance in the level of correlation of noisy signals. Note, however, that the fact that the average time lag between signals is generally very low means that there is no large systematic time lag between most sites. It does not mean that there is no time lag between activity of sites at the level of individual call events, but if it exists, it is variable.

Another interesting pattern that arises from the latency-sorted raster plots in Figures 9 and 10, is that deviant events do not appear to be distributed uniformly along the sorting gradient of epochs that contain responses (see color bars at the right side of the rasters): deviants tend to be more common toward the top of the raster plots, which means they have a relatively short peak latency. Figure 9*G* illustrates this difference in latency between standard and deviant calls. We tested for the sites of which we manually determined response thresholds (see above) whether or not those epochs that contain response activity differ in peak latency between deviant and standard events. This is indeed the case: deviant events generally have shorter peak latencies than standard events (medians of 195 and 237 ms, respectively; LMM, dependent variable peak latency, fixed factor probability, $t = 5.5$, $p < 0.0001$). This shows that the internally synchronized network activity is part of, or is linked to, the neural circuits underlying auditory deviance detection.

We tested for an effect of the level of synchronicity (IS; fixed factor) on deviant preference (DP_C; dependent variable), for secondary sites, and this effect turns out to be significant (LMM; $t = 2.2$, $p = 0.03$). However, we cannot exclude that this relationship is simply based on sites with stronger responses yielding higher cross-covariance (IS) and higher DP_C values because these sites have a better signal-to-noise ratio. Future work based on single-unit measurements should confirm this result.

Discussion

Our results show that auditory responses of many sites in the medial parts of the secondary auditory forebrain (medial parts of NCM and CMM) show a strong bias to calls that deviate from those that are expected on the basis of recent stimulus history. The majority of such sites are sensitive to deviance of multiple call stimuli. This type of deviance sensitivity is not simply based on auditory change with respect to the most recent stimulus, but must involve memory traces of multiple past stimuli. Furthermore, we find that standard calls are often not responded to. Primary auditory sites (L2), in contrast, are not strongly sensitive to call deviance and respond to all occurrences of a call stimulus. Last, we found that responses at secondary auditory sites are to a large extent internally synchronized. When one site does not respond, often many other secondary sites do not respond. And when a site does respond, its response pattern is similar to that of many other sites, including distant ones.

Overall, our findings suggest that, in the normal sensory environment of zebra finches, which is rife with often-repeated contact calls from group members (Beckers and Gahr, 2010; Elie et al., 2011), neural processing of "standard" calls is mostly limited to the thalamorecipient layer L2. "Deviant calls," in contrast, elicit much more widespread activity that includes the medial parts of the secondary auditory areas CMM an NCM. The fact that responses differ between primary and secondary areas in terms of event-to-event stereotypy and internal synchronization, suggests that deviant calls do not simply stimulate a larger part of a single network, but rather activate an additional and different kind of network in downstream processing areas. Given that this deviance-dependent activity may be completely absent during many call events, and thus is not strongly linked to sensory coding, and given that it is present under anesthesia, it may reflect an early-stage process that is involved in the involuntary capturing of attention. This is also a suggested function of the mechanisms that underlie the EEG recorded MMN in humans (Escera et al., 1998), which is usually recorded in awake human subjects, but has also been shown to occur under deep anesthesia (Koelsch et al., 2006) and during sleep (Sculthorpe et al., 2009).

In general, the simplest mechanism that could underlie a response bias to a rare stimulus would be based on a use-dependent

←

(*Figure legend continued.*) randomly timed with respect to call occurrence it would show a linear shape. This is illustrated here by superposing a semitransparent version of the call triggered activity raster of site (2,2) in ***C*** (in gray tones) on an activity raster of the same activity but then randomly triggered (in green tones; random uniform distribution, for each event between 0 and 625 ms after call occurrence). ***G***, The latency of the peak activity bursts differs depending on whether or not a call stimulus is deviant. Note that the time axis of the two rasters ranges from 0 to 150 ms after call onset for visual purposes but that quantification of peak latency was based on the complete response epoch duration of 625 ms. The bottom plot shows the latency of the peak activity (i.e., maximum AMUA within an epoch) extracted from the top rasters, a procedure that was used to statistically test for differences in latency between standard and deviant conditions across all birds in this study, the outcome of which is highly significant (see Results, Responses of secondary auditory sites are internally synchronized).

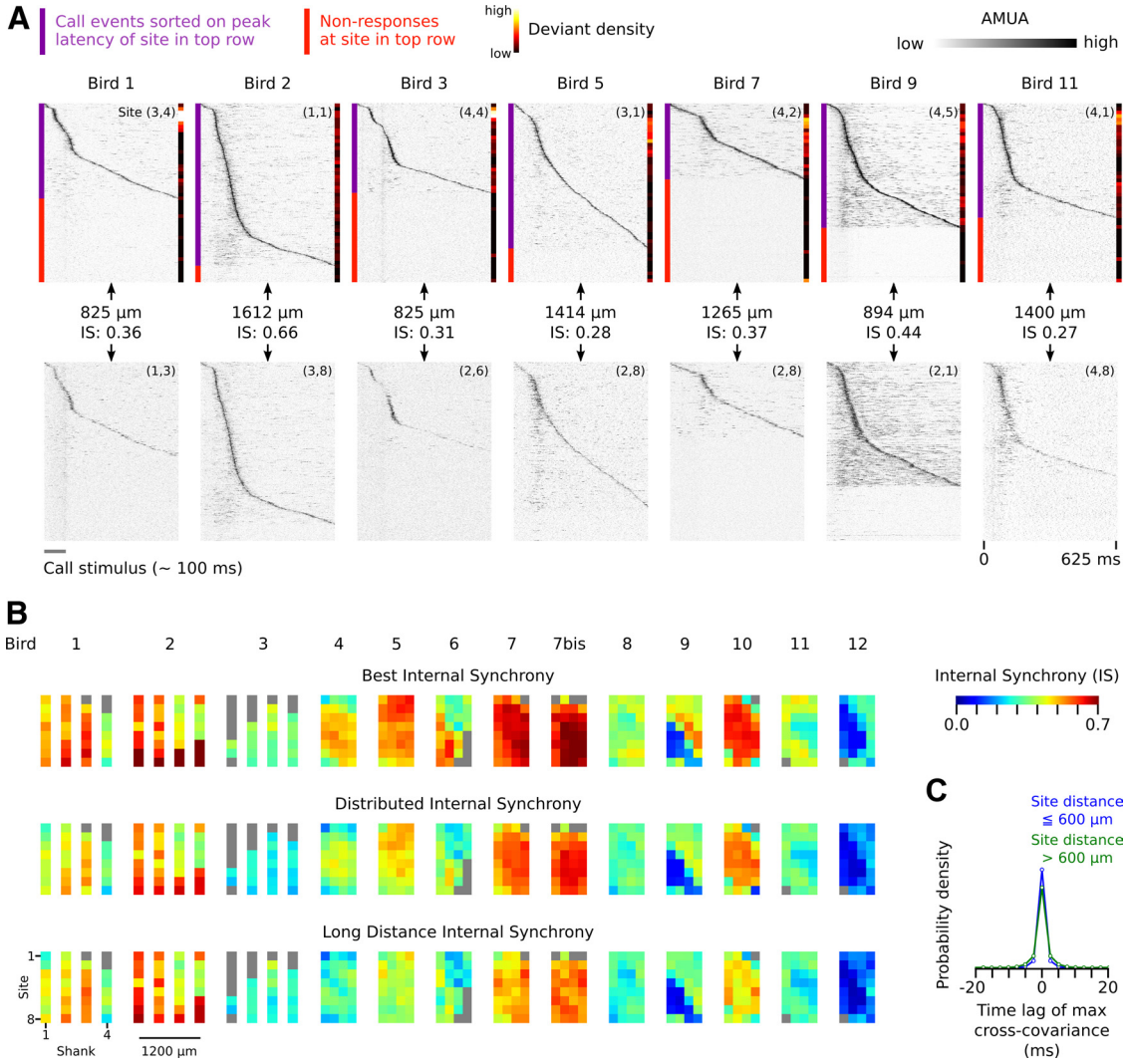

Figure 10. ***A***, Additional examples of synchronous activity between secondary auditory sites that are separated by large distances. For each bird, raster plots are sorted from top to bottom on the latency of the strongest peak in the AMUA signal of the site in the top row. The events in the raster plots of the sites in the bottom row are aligned to those of the raster plot in the top row. Note that the pattern of peak activity in the top row often matches to activity at the site in the bottom row, and that nonresponses in the top row correspond to nonresponses in the bottom row. Also note that deviant events, the density of which is indicated by the color bar on the right side of raster plots, tend to have lower peak latencies (i.e., occur more frequently toward the top of the raster plot). ***B***, Image plots of mean IS indices for all sites in this study. Each colored pixel represents the mean of the IS of that site (for anatomical location of sites, see Fig. 3) with a selection of other sites. Each row of image plots corresponds to a different kind of selection. In the top row (IS_B), the mean is calculated over the four highest IS values; in the middle row (IS_D), it is calculated over the 16 highest IS values; in the bottom row (IS_L), it is calculated over the 4 highest IS values between the focal site and sites that are at least separated by 600 μm from the focal site. Gray pixels are sites that either were generally unresponsive or did not have sufficient concurrent responses with other sites (<5% of epochs). ***C***, Distribution of time lags of maximum normalized cross-covariance between secondary auditory site pairs. Site pairs have been categorized depending on whether or not the distance between them is >600 μm. For most site pairs, cross-covariance is maximal at 0.0 ms.

reduction of neuronal firing (fatigue) in response to repeated sensory stimulation (Nelken and Ulanovsky, 2007). However, such a simple use-dependent mechanism takes place at the integration level of a neuron and is difficult to reconcile with our finding that deviant preferences are generally positive, and often large, for both call stimuli in a series. It may be argued that multiunit activity recorded at a site originates from distinct neuronal sources, each responding in a use-dependent way to an acoustic feature that is not shared between the two stimuli. If so, most sites in the medial secondary auditory forebrain would consist of neurons that are closely associated spatially but that at the same time are very narrowly tuned to different acoustic features. However, this is not compatible with the finding that, between many sites, responses are synchronized, and are variable in response latency to acoustically identical stimuli. Together, a mechanism based on fatigue from sensory stimulation is not supported by the observations, and a more complex mechanism must underlie the deviance-sensitive activity in secondary auditory areas. This mechanism is sensitive to acoustic deviance per se and could be used to detect rare vocalizations in natural communication scenes.

Sensitivity to auditory deviance, or surprise, has recently also been found in the caudal lateral mesopallium (CLM) of zebra finches (Gill et al., 2008). However, this phenomenon was observed on much shorter timescales (<10 ms) than the one used in the current study (625 ms), and was based on constituent acoustic features, not complete vocalizations. In contrast to our findings in the more medially situated CMM and NCM, these authors did not find any evidence of response variation between recurring vocalizations in CLM. Although there are multiple methodological differences with the present study, which complicate the drawing of firm conclusions on this issue, it may well be that

responses in CLM are distinctly different with respect to the temporal scale of stimulus history sensitivity from those in the medial parts of CMM and NCM. Some support for this hypothesis is provided by the recent finding that in starlings, *Sturnus vulgaris*, CMM neurons show more variable responses to repeated components of song than CLM neurons do (Jeanne et al., 2011).

A different type of sensitivity to auditory deviance has very recently been found in the optic tectum of barn owls (*Tyto alba*). This phenomenon is relatively long-lasting (up to 60 s) and operates both on artificial and natural stimuli (Netser et al., 2011). Its relationship with the type of sensitivity found in the present study remains as yet unclear because of differing stimulation paradigms; it may be that they represent two different mechanisms, but it may also be that secondary auditory forebrain circuits compute novelty of sound objects in natural auditory scenes and modulate tectal responses (Netser et al., 2011).

The stimulus specificity of the responses at secondary auditory sites is reminiscent of SSA in mammals (Ulanovsky et al., 2003). However, we agree with Nelken and Ulanovsky (2007) that it is problematic to directly compare observations in studies using pure tone stimuli and simple deviations in one dimension, which is how SSA is measured, with those from studies using natural stimuli differing in complex ways. Therefore, the term "SSA" is probably best reserved for stimulus-specific habituation to tone stimuli. Nevertheless, phenomenologically, another parallel between the deviance sensitivity identified in the current study and SSA is that responses need not occur to every stimulus event. This has also been reported for SSA in cats (Ulanovsky et al., 2004), where, like in the current study, nonresponses contribute strongly to response strength differences between standard and deviant stimuli. One important difference, however, is that nonresponses in cats were found in primary auditory cortex (A1), layer 4 of which is believed to be functionally similar to the avian L2 (Wang et al., 2010), where we did not find nonresponses (in multiunit signals).

The use of multielectrodes enabled us to show directly that there are at least two different mechanisms underlying response modulation when call stimuli recur at a natural rate. First, in L2, a sensory-adaptation type of mechanism modulates response strength in a way that is not, or only weakly, call stimulus specific, which is in line with earlier findings (Beckers and Gahr, 2010). Recent work has shown that neurons in L2 also show short-term adaptation to pure tone sounds [starlings, *S. vulgaris* (Bee and Klump, 2004, 2005; Bee et al., 2010)] and to noise sounds with natural amplitude modulation characteristics [zebra finches (Nagel and Doupe, 2006; Sharpee et al., 2011)]. Second, a different mechanism that is sensitive to call deviance is manifest in the higher-order auditory areas NCM and CMM, which may be comparable in function to higher-order auditory cortices in mammals (Bolhuis and Gahr, 2006). The properties of this mechanism are different because of the large-scale internal synchronization between many sites, and because responses are not obligatory and have variable latencies to identical stimuli. Such properties are often associated with perceptual processes rather than sensory ones. Whether or not the mechanism present in secondary auditory areas is functionally similar to the hypothesized model-building component of MMN (for review, see Garrido et al., 2009) is an issue that should be investigated in a future study, for example by using a "deviant-within-many-standards" design (Schröger and Wolff, 1996; Farley et al., 2010).

To our knowledge, the internal synchrony that we found between sites in the medial parts of secondary auditory areas has not been described before in other auditory studies in birds, or in SSA studies in mammals. It cannot be excluded that the extent of synchrony we found is dependent on the use of anesthesia, and may be reduced or even absent in the awake state. Nevertheless, the fact that the latency of peak activity, which is synchronized between sites, is sensitive to call deviance shows that this type of activity is involved in the neural processing of context-dependent auditory information. Previously, Sutter and Margoliash (1994) reported in anesthetized male zebra finches synchronous responses to the bird's own song across sites within HVC, a premotor song nucleus that also has auditory properties, but the synchrony of these responses was strongly linked to the timing of the external stimulus and may therefore represent a form of external synchronization. Furthermore, Janata and Margoliash (1999) directly recorded correlated activity bursts between HVC and nucleus interfacialis (NIf) in anesthetized male zebra finches, but that activity could not be linked to a functional process and its origin (external/internal) is unknown. Although it is clear that the cause of synchrony in the deviance-dependent responses that we found across the medial parts of NCM and CMM is not related to the timing of stimulus acoustic features, and thus must arise from internal interactions, it remains unclear how exactly it comes about. It may arise from interactions within the secondary auditory forebrain, but, given the very short latency differences between sites, it may also arise from an upstream, common source in the thalamus or brainstem. The fact that responses in L2, which projects directly to NCM and indirectly to CMM (Vates et al., 1996; Smith et al., 2006), are not internally synchronized does not preclude an upstream source because there are direct connections from the "shell" of the thalamic nucleus ovoidalis (Ov) to NCM that bypass L2 (Vates et al., 1996).

Together, our study shows that synchronized neuronal networks in the medial secondary auditory forebrain of zebra finches are sensitive to deviance in the short-term delivery patterns of call vocalizations. Future work should specifically address how internal synchronicity comes about, and whether or not the activity of this network reflects the strength of a short-term memory representation of current input, or, as has been hypothesized for MMN in humans, a mismatch between predicted and actual input.

References

Amin N, Doupe A, Theunissen FE (2007) Development of selectivity for natural sounds in the songbird auditory forebrain. J Neurophysiol 97:3517–3531.

Anderson LA, Christianson GB, Linden JF (2009) Stimulus-specific adaptation occurs in the auditory thalamus. J Neurosci 29:7359–7363.

Antunes FM, Nelken I, Covey E, Malmierca MS (2010) Stimulus-specific adaptation in the auditory thalamus of the anesthetized rat. PLoS One 5:e14071.

Baayen R, Davidson D, Bates D (2008) Mixed-effects modeling with crossed random effects for subjects and items. J Mem Lang 59:390–412.

Beckers GJ, Gahr M (2010) Neural processing of short-term recurrence in songbird vocal communication. PLoS One 5:e11129.

Bee MA, Klump GM (2004) Primitive auditory stream segregation: a neurophysiological study in the songbird forebrain. J Neurophysiol 92:1088–1104.

Bee MA, Klump GM (2005) Auditory stream segregation in the songbird forebrain: effects of time intervals on responses to interleaved tone sequences. Brain Behav Evol 66:197–214.

Bee MA, Micheyl C, Oxenham AJ, Klump GM (2010) Neural adaptation to tone sequences in the songbird forebrain: patterns, determinants, and relation to the build-up of auditory streaming. J Comp Physiol A 196:543–557.

Blanche TJ, Spacek MA, Hetke JF, Swindale NV (2005) Polytrodes: high-density silicon electrode arrays for large-scale multiunit recording. J Neurophysiol 93:2987–3000.

Bolhuis JJ, Gahr M (2006) Neural mechanisms of birdsong memory. Nat Rev Neurosci 7:347–357.

Chew SJ, Vicario DS, Nottebohm F (1996) A large-capacity memory system

that recognizes the calls and songs of individual birds. Proc Natl Acad Sci U S A 93:1950–1955.
Cousillas H, Leppelsack HJ, Leppelsack E, Richard JP, Mathelier M, Hausberger M (2005) Functional organization of the forebrain auditory centres of the European starling: a study based on natural sounds. Hear Res 207:10–21.
Csicsvari J, Henze DA, Jamieson B, Harris KD, Sirota A, Barthó P, Wise KD, Buzsáki G (2003) Massively parallel recording of unit and local field potentials with silicon-based electrodes. J Neurophysiol 90:1314–1323.
Elie JE, Soula HA, Mathevon N, Vignal C (2011) Dynamics of communal vocalizations in a social songbird, the zebra finch (*Taeniopygia guttata*). J Acoust Soc Am 129:4037–4046.
Escera C, Alho K, Winkler I, Näätänen R (1998) Neural mechanisms of involuntary attention to acoustic novelty and change. J Cogn Neurosci 10:590–604.
Farley BJ, Quirk MC, Doherty JJ, Christian EP (2010) Stimulus-specific adaptation in auditory cortex is an NMDA-independent process distinct from the sensory novelty encoded by the mismatch negativity. J Neurosci 30:16475–16484.
Fortune ES, Margoliash D (1992) Cytoarchitectonic organization and morphology of cells of the field L complex in male zebra finches (*Taenopygia guttata*). J Comp Neurol 325:388–404.
Fortune ES, Margoliash D (1995) Parallel pathways and convergence onto HVc and adjacent neostriatum of adult zebra finches (*Taeniopygia guttata*). J Comp Neurol 360:413–441.
Garrido MI, Kilner JM, Stephan KE, Friston KJ (2009) The mismatch negativity: a review of underlying mechanisms. Clin Neurophysiol 120:453–463.
Gill P, Woolley SM, Fremouw T, Theunissen FE (2008) What's that sound? Auditory area CLM encodes stimulus surprise, not intensity or intensity changes. J Neurophysiol 99:2809–2820.
Grace JA, Amin N, Singh NC, Theunissen FE (2003) Selectivity for conspecific song in the zebra finch auditory forebrain. J Neurophysiol 89:472–487.
Janata P, Margoliash D (1999) Gradual emergence of song selectivity in sensorimotor structures of the male zebra finch song system. J Neurosci 19:5108–5118.
Jeanne JM, Thompson JV, Sharpee TO, Gentner TQ (2011) Emergence of learned categorical representations within an auditory forebrain circuit. J Neurosci 31:2595–2606.
Koelsch S, Heinke W, Sammler D, Olthoff D (2006) Auditory processing during deep propofol sedation and recovery from unconsciousness. Clin Neurophysiol 117:1746–1759.
Malmierca MS, Cristaudo S, Pérez-González D, Covey E (2009) Stimulus-specific adaptation in the inferior colliculus of the anesthetized rat. J Neurosci 29:5483–5493.
Meliza CD, Chi Z, Margoliash D (2010) Representations of conspecific song by starling secondary forebrain auditory neurons: toward a hierarchical framework. J Neurophysiol 103:1195–1208.
Müller CM, Leppelsack HJ (1985) Feature extraction and tonotopic organization in the avian auditory forebrain. Exp Brain Res 59:587–599.
Näätänen R (2003) Mismatch negativity: clinical research and possible applications. Int J Psychophysiol 48:179–188.
Näätänen R, Tervaniemi M, Sussman E, Paavilainen P, Winkler I (2001) "Primitive intelligence" in the auditory cortex. Trends Neurosci 24:283–288.
Näätänen R, Paavilainen P, Rinne T, Alho K (2007) The mismatch negativity (MMN) in basic research of central auditory processing: a review. Clin Neurophysiol 118:2544–2590.
Nagel KI, Doupe AJ (2006) Temporal processing and adaptation in the songbird auditory forebrain. Neuron 51:845–859.
Nelken I, Ulanovsky N (2007) Mismatch negativity and stimulus-specific adaptation in animal models. J Psychophysiol 21:214–223.
Netser S, Zahar Y, Gutfreund Y (2011) Stimulus-specific adaptation: can it be a neural correlate of behavioral habituation? J Neurosci 31:17811–17820.
Pérez-González D, Malmierca MS, Covey E (2005) Novelty detector neurons in the mammalian auditory midbrain. Eur J Neurosci 22:2879–2885.
Phan ML, Pytte CL, Vicario DS (2006) Early auditory experience generates long-lasting memories that may subserve vocal learning in songbirds. Proc Natl Acad Sci U S A 103:1088–1093.
R Development Core Team (2009) R: a language and environment for statistical computing. Vienna: R Foundation for Statistical Computing.
Schröger E, Wolff C (1996) Mismatch response of the human brain to changes in sound location. Neuroreport 7:3005–3008.
Sculthorpe LD, Ouellet DR, Campbell KB (2009) MMN elicitation during natural sleep to violations of an auditory pattern. Brain Res 1290:52–62.
Shaevitz SS, Theunissen FE (2007) Functional connectivity between auditory areas field L and CLM and song system nucleus HVC in anesthetized zebra finches. J Neurophysiol 98:2747–2764.
Sharpee TO, Nagel KI, Doupe AJ (2011) Two-dimensional adaptation in the auditory forebrain. J Neurophysiol 106:1841–1861.
Singer W (1999) Neuronal synchrony: a versatile code for the definition of relations? Neuron 24:49–65.
Smith VA, Yu J, Smulders TV, Hartemink AJ, Jarvis ED (2006) Computational inference of neural information flow networks. PLoS Comput Biol 2:e161.
Squires KC, Wickens C, Squires NK, Donchin E (1976) The effect of stimulus sequence on the waveform of the cortical event-related potential. Science 193:1142–1146.
Sutter ML, Margoliash D (1994) Global synchronous response to autogenous song in zebra finch HVc. J Neurophysiol 72:2105–2123.
Theunissen FE, Sen K, Doupe AJ (2000) Spectral-temporal receptive fields of nonlinear auditory neurons obtained using natural sounds. J Neurosci 20:2315–2331.
Uhlhaas PJ, Pipa G, Lima B, Melloni L, Neuenschwander S, Nikolić D, Singer W (2009) Neural synchrony in cortical networks: history, concept and current status. Front Integr Neurosci 3:17.
Ulanovsky N, Las L, Nelken I (2003) Processing of low-probability sounds by cortical neurons. Nat Neurosci 6:391–398.
Ulanovsky N, Las L, Farkas D, Nelken I (2004) Multiple time scales of adaptation in auditory cortex neurons. J Neurosci 24:10440–10453.
Vates GE, Broome BM, Mello CV, Nottebohm F (1996) Auditory pathways of caudal telencephalon and their relation to the song system of adult male zebra finches (*Taenopygia guttata*). J Comp Neurol 366:613–642.
Venables WN, Ripley BD (1999) Modern applied statistics with S-PLUS. New York: Springer.
von der Behrens W, Bäuerle P, Kössl M, Gaese BH (2009) Correlating stimulus-specific adaptation of cortical neurons and local field potentials in the awake rat. J Neurosci 29:13837–13849.
Wang Y, Brzozowska-Prechtl A, Karten HJ (2010) Laminar and columnar auditory cortex in avian brain. Proc Natl Acad Sci U S A 107:12676–12681.
Winkler I (2007) Interpreting the mismatch negativity. J Psychophysiol 21:147–163.
Winkler I, Teder-Sälejärvi WA, Horváth J, Näätänen R, Sussman E (2003) Human auditory cortex tracks task-irrelevant sound sources. Neuroreport 14:2053–2056.
Yu XJ, Xu XX, He S, He J (2009) Change detection by thalamic reticular neurons. Nat Neurosci 12:1165–1170.
Zann RA (1996) The zebra finch. New York: Oxford UP.